Electronic Supplementary Information

Molecular Ru(II) complexes with universal pH hydrogen evolution performance

Rakesh Kumar,[a] Baghendra Singh,[a] and Apparao Draksharapu[a,*]

[a]Southern Laboratories-208A, Department of Chemistry, Indian Institute of Technology Kanpur, Kanpur–208016 (India).

Experimental Section

Materials and Methods:

All chemicals and reagents were obtained from commercial sources and were used as received. HPLC-grade H_2O and CH_3CN from Merck were used in the spectroscopic studies. The elemental analysis (C, H, N) was performed using a Perkin Elmer CHNS/O 2400 series II Analyser. The FT-IR (KBr, 4000–500 cm^{-1}) spectrum of **1** and **2** was acquired on a Perkin Elmer Spectrum Two spectrometer. An Agilent 8453 diode-array spectrophotometer was used to record the UV/Vis absorption spectra and conduct the kinetic experiments spectrophotometrically in 1 cm quartz cells (λ = 200–1000 nm range). The ESI-MS was recorded on an Agilent 6546 LC/Q-TOF in the positive-ion mode. The ^{1}H and ^{13}C NMR spectra were obtained using JEOL JNM LA 500 (500 MHz) and JEOL JNM LA 400 (400 MHz) NMR spectrometers. The cyclic voltammetry experiments were carried out at room temperature using a CH Instruments Electrochemical Analyzer M-600B series. A three-electrode system was used, with glassy carbon as the working electrode, Pt wire as the auxiliary electrode, and aqueous Ag/AgCl as the reference electrode. The solutions used were 1 mM **1** (and **2**) and 100 mM supporting electrolyte tetra-*n*-butylammonium hexafluorophosphate ($TBAPF_6$) in acetonitrile and sodium perchlorate in water. All spectroscopy experiments in this work were carried out under aerobic conditions unless stated otherwise.

X-ray crystallography

A single crystal of suitable dimensions was used for data collection. Diffraction intensities were collected on a Bruker D8 Venture Duo X-ray diffractometer and software suite CCD diffractometer, with graphite-monochromated Mo Kα (0.71073 Å) radiation at 100 K. Data were corrected for Lorentz and polarization effects; empirical absorption corrections (SADABS v 2.10) were applied. Using Olex2,[1] the structures were solved by ShelXT[2] structure solution program using Intrinsic Phasing and refined with the ShelXL[3] refinement package using Least Squares minimization. The non-hydrogen atoms were refined anisotropically, whereas the H atoms fixed to their geometrically ideal positions were refined isotropically. CCDC **2426238** and **2426239** contain the supplementary crystallographic data for **1** and **2**, respectively. This data can be obtained free of charge from the Cambridge Crystallographic Data Centre *via* www.ccdc.cam.ac.uk.

Synthesis of N^1-benzyl-N^1,N^2,N^2-tris((1-methyl-1H-benzo[d]imidazol-2-yl)methyl)ethane-1,2-diamine (BnTBEN): Synthesis of the ligand was carried out using our reported method.[4]

Synthesis of $[Ru^{II}(BnTBEN)(NCCH_3)](PF_6)_2$ (1)

Synthesis of **1** was carried out by following a literature procedure for the synthesis of $[Ru^{II}(BnTPEN)(NCCH_3)](PF_6)_2$.[5] A mixture of BnTBEN (380 mg, 0.65 mmol), ruthenium(III) chloride hydrate ($RuCl_3 \cdot xH_2O$) (300 mg, 1.45 mmol), and *L*-ascorbic acid (230 mg, 1.30 mmol) was heated under reflux overnight in 20 mL of EtOH and 30 mL of the H_2O mixture. The reaction mixture was cooled to room temperature. The solvent was completely removed under vacuum. The crude product was purified by column chromatography on neutral alumina, eluting with CH_3CN to yield the $[Ru^{II}(BnTBEN)(Cl)](Cl)$ complex. Saturated aqueous potassium hexafluorophosphate (KPF_6) was added to $[Ru^{II}(BnTBEN)(Cl)](Cl)$ in water, which resulted in $[Ru^{II}(BnTBEN)(Cl)](PF_6)$ as a red solid. This red solid was left to dry overnight under a high vacuum, after which it was redissolved in 30 mL of acetonitrile and 3 mL of water. This mixture was heated overnight at 60 °C. The reaction mixture was then cooled to room temperature, and the solvent was reduced to 4–5 mL under vacuum. A few

drops of saturated aqueous KPF_6 were subsequently added to the solution to yield **1** as a red solid (210 mg, 32%). Single crystals suitable for X-ray analysis were obtained by the slow vapor diffusion of diethyl ether into the acetonitrile solution of **1** at room temperature overnight. ^{1}H NMR (400 MHz, CD_3CN): δ (ppm) 8.26 (d, 1H, J = 8.2 Hz), 7.72 (d, 1H, J = 8.04 Hz), 7.61 (d, 1H, J = 8.36 Hz), 7.54 (d, 1H, J = 8.32 Hz), 7.48 (d, 1H, J = 8.04 Hz), 7.46 – 7.34 (m, 9H), 7.30 – 7.25 (m, 2H), 6.87 (t, 1H, J = 8.24 Hz), 5.43 (d, 1H, J = 8.28 Hz), 4.86 – 4.64 (m, 3H), 4.51 (t, 2H, J = 14.0 Hz), 3.97 – 3.90 (m, 2H), 3.83 (s, 3H), 3.78 (s, 3H), 3.69 (s, 3H), 3.44 (t, 2H, J = 12.72 Hz), 3.08 (t, 2H, J = 13.72 Hz), 2.65 (s, 3H). ^{13}C NMR (125 MHz, CD_3CN): δ (ppm) 158.21, 156.96, 156.39, 143.58, 132.58, 132.34, 129.98, 129.65, 125.27, 124.83, 124.73, 124.56, 124.51, 115.56, 112.71, 112.37, 111.80, 70.28, 65.83, 63.17, 61.60, 59.51, 32.64, 32.46, 5.35. ESI-MS: m/z 870.22 $[Ru^{II}(BnTBEN)(NCCH_3)(PF_6)]^+$. Anal. Calc. for $RuC_{38}H_{41}N_9P_2F_{12}.2H_2O$: C, 43.43; N, 12.00; H, 4.32. Found: C, 42.95; N, 11.90; H, 4.13.

Synthesis of N^1-methyl-N^1,N^2,N^2-tris((1-methyl-1H-benzo[d]imidazol-2-yl)methyl)ethane-1,2-diamine (MeTBEN): 2-(chloromethyl)-1-methyl-1H-benzo[d]imidazole (4.4 g, 24.3 mmol) was dissolved in 15 mL of water followed by N^1-methylethane-1,2-diamine (700 µL, 8.1 mmol) in a round-bottom flask equipped with a stir bar. Aqueous NaOH solution (930 mg, 24.3 mmol) was slowly added dropwise over an hour. The resulting mixture was stirred at room temperature for 7 days. The reaction mixture was extracted three times with 25 mL of methylene chloride. The combined organic phases were dried over Na_2SO_4, and the solvent was evaporated under reduced pressure. Yield: 2.67 g (65 %). Characterization: ^{1}H NMR (400 MHz, $CDCl_3$) δ (ppm) 7.69 – 7.67 (m, 3H), 7.25 – 7.21 (m, 7H), 7.17 – 7.14 (m, 2H), 4.04 (s, 4H), 3.88 (s, 2H), 3.59 (s, 2H), 3.50 (s, 6H), 2.97 (t, 2H, J = 6.34 Hz), 2.83 (t, 2H, J = 6.24 Hz), 2.33 (s, 3H). ^{13}C NMR (100 MHz, $CDCl_3$) δ (ppm) 151.64, 151.17, 135.93, 129.39, 128.35, 127.47, 122.97, 122.34, 118.56, 119.25, 109.42, 109.33, 59.61, 52.62, 51.76, 51.49, 51.35, 30.00, 29.68.

Synthesis of [Ru^{II}(MeTBEN)($NCCH_3$)](PF_6)$_2$ (2)

Synthesis of **2** was carried out by following a literature procedure for the synthesis of [Ru^{II}(BnTPEN)($NCCH_3$)](PF_6)$_2$.[5] A mixture of MeTBEN (405 mg, 0.80 mmol), ruthenium(III) chloride hydrate ($RuCl_3 \cdot xH_2O$) (375 mg, 1.80 mmol), and *L*-ascorbic acid (285 mg, 1.60 mmol) was heated under reflux overnight in 20 mL of EtOH and 30 mL of the H_2O mixture. The reaction mixture was cooled to room temperature. The solvent was completely removed under vacuum. The crude product was purified by column chromatography on neutral alumina, eluting with CH_3CN to yield the [Ru^{II}(MeTBEN)(Cl)](Cl) complex. Saturated aqueous potassium hexafluorophosphate (KPF_6) was added to [Ru^{II}(MeTBEN)(Cl)](Cl) in water, which resulted in [Ru^{II}(MeTBEN)(Cl)](PF_6) as a red solid. This red solid was left to dry overnight under a high vacuum, after which it was redissolved in 30 mL of acetonitrile and 3 mL of water. This mixture was heated overnight at 60 °C. The reaction mixture was then cooled to room temperature, and the solvent was reduced to 4–5 mL under vacuum. A few drops of saturated aqueous KPF_6 were subsequently added to the solution to yield **2** as a red solid (220 mg, 30%). Single crystals suitable for X-ray analysis were obtained by the slow vapor diffusion of diethyl ether into the acetonitrile solution of **2** at room temperature overnight. ^{1}H NMR (500 MHz, CD_3CN): δ (ppm) 8.20 (d, 1H, J = 8.10 Hz), 7.70 (d, 1H, J = 8.15 Hz), 7.62 (d, 1H, J = 8.30 Hz), 7.58 (d, 1H, J = 8.25 Hz), 7.48 – 7.44 (m, 3H), 7.40 – 7.36 (m, 2H), 7.30 – 7.27 (m, 2H), 6.89 – 6.86 (m, 1H), 5.46 (d, 1H, J = 8.25 Hz), 4.90 (d, 1H, J = 15.55 Hz), 4.63 (d, 1H, J = 19.15 Hz), 4.52 (d, 3H, J = 16.7 Hz), 3.87 (s, 3H), 3.85 (s, 3H), 3.64 (s, 3H), 3.42 – 3.40 (m, 2H), 3.35 – 3.32 (m, 2H), 2.71 (s, 3H) 2.60 (s, 3H). ^{13}C NMR (125 MHz, CD_3CN): δ (ppm) 157.72, 156.42, 155.93, 143.21, 143.09, 141.69, 136.37, 135.92, 124.77, 124.31, 124.22, 124.03, 123.99, 115.0, 111.31, 68.08, 62.74, 62.56, 62.48, 60.90, 53.75, 32.08, 31.98, 31.79, 4.54. ESI-MS: m/z 794.19 [Ru^{II}(MeTBEN)($NCCH_3$)(PF_6)]$^+$. Anal. Calc. for $RuC_{32}H_{37}N_9P_2F_{12}.2CH_3CN$: C, 42.36; N, 15.09; H, 4.25. Found: C, 42.50; N, 15.20; H, 4.15.

The complex **2**, [(MeTBEN)Ru^{II}($NCCH_3$)](PF_6)$_2$, exhibits intense absorption bands at 277 nm ($\varepsilon_{277\ nm}$ = 7,040 $M^{-1}cm^{-1}$), 325 nm ($\varepsilon_{325\ nm}$ = 3,760 $M^{-1}cm^{-1}$), and at 468 nm ($\varepsilon_{468\ nm}$ = 210 $M^{-1}cm^{-1}$) in acetonitrile (Fig. 2B and S5B). The

ESI-MS analysis of **2** displayed three major peaks corresponding to the ions $[(MeTBEN)Ru^{II}(NCCH_3)(PF_6)]^+$ (m/z: 794.1861), $[(MeTBEN)Ru^{II}(F)]^+$ (m/z: 627.1934) and $\{Na[(BnTBEN)Ru^{II}(NCCH_3)(PF_6)_2]\}^+$ (m/z: 962.1391), corroborating the presence of a Ru(II) complex in acetonitrile solution (Fig. S10). Complex **2** crystallized in the monoclinic crystal system with the space group $P2_1/n$. The crystal structure reveals that the Ru(II) ion coordinates with the five nitrogen atoms of the MeTBEN ligand, while the sixth coordination site accommodates a solvent $NCCH_3$ molecule, resulting in a distorted octahedral geometry. Two PF_6^- anions serve as counterions in the asymmetric unit. The benzimidazole ring nitrogens in the ligand occupy the equatorial plane, with bond lengths to N3, N4, and N5 from Ru measuring 2.068(3) Å, 2.58(3) Å, and 2.057(3) Å, respectively. The two amine nitrogens are positioned at the equatorial and axial sites, with bond lengths to N1 and N2 from Ru at 2.105(3) Å and 2.149(3) Å, respectively. The sixth site is filled by the $NCCH_3$ molecule, forming a Ru–N6 bond length of 2.022(3) Å. The average Ru–N bond distance of 2.08 Å aligns well with a Ru(II) low-spin complex. In the asymmetric unit of the crystal structure of **2**, there is one Ru(II) ion, one MeTBEN ligand, one $NCCH_3$ molecule, and two PF_6^- anions, along with two $NCCH_3$ solvent molecules (Fig. 1B, Tables S1 and S2). ^{1}H NMR spectrum of **2** in CD_3CN exhibits signals in the diamagnetic region, further confirming the low-spin nature of the Ru(II) center in solution (Fig. S11 and S12). A distinct vibrational band at 2255 cm^{-1} observed in the FT-IR spectrum of **2** (Fig. S13) corresponds to the bound acetonitrile ligand at the sixth coordination site. A reversible redox wave with $E_{1/2}$ = 0.77 V vs. Ag/AgCl observed in its cyclic voltammetry corresponds to the Ru(III)/Ru(II)($NCCH_3$) redox couple in acetonitrile (Fig. 2A).

Fabrication of the complexes on carbon cloth:

The complexes **1** and **2** (4 mg) were dissolved in 50 µL of acetonitrile, and 10 µL of a 0.05 wt% Nafion solution in ethanol was added. The mixture was sonicated for 10 min. The suspension was then drop-casted on carbon cloth (geometrical surface area, 1 cm^2). Electrochemistry HER activity was investigated using complexes on carbon cloth as a working electrode.

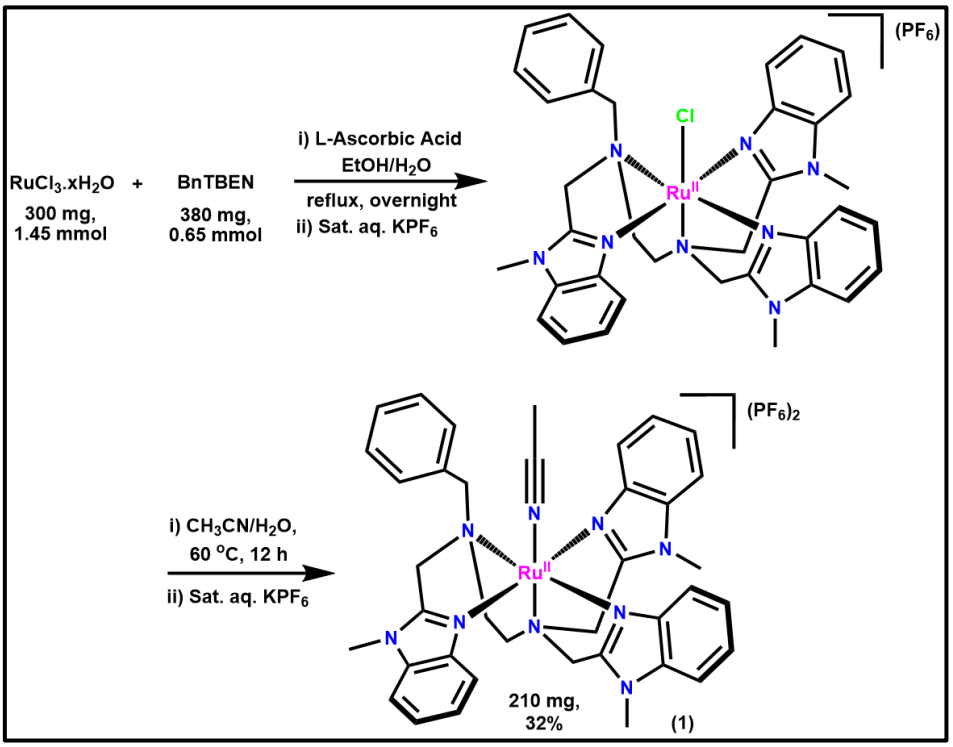

Scheme S1: Synthetic procedure for $[Ru^{II}(BnTBEN)(NCCH_3)](PF_6)_2$ (**1**).

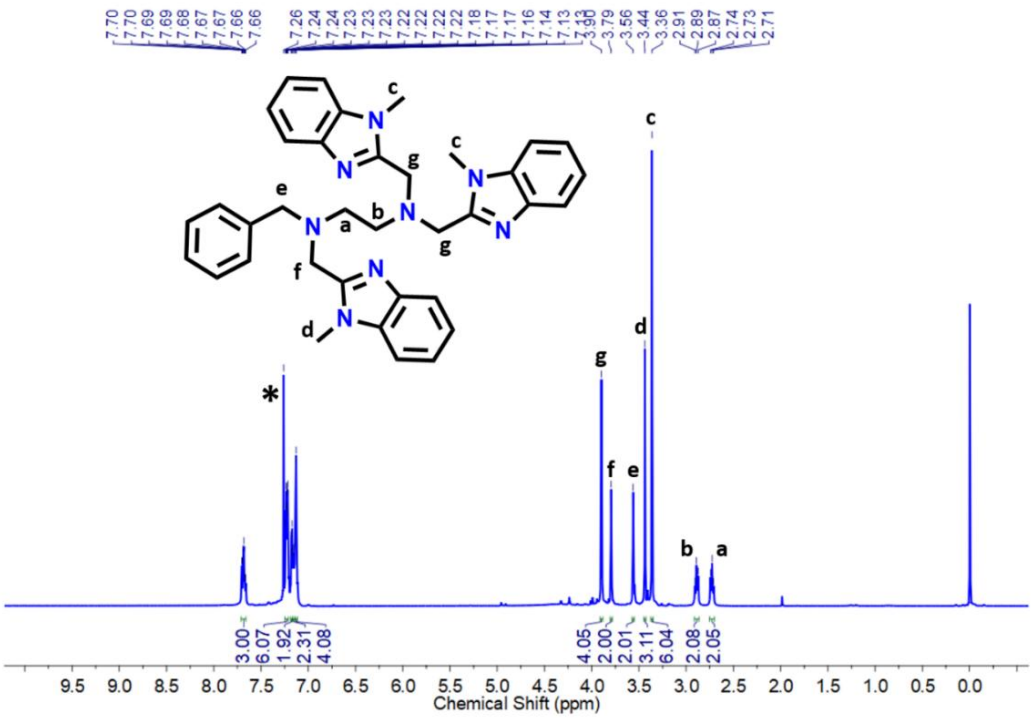

Figure S1: ^1H NMR spectrum of BnTBEN in $CDCl_3$ at 400 MHz. (* peak for solvent).

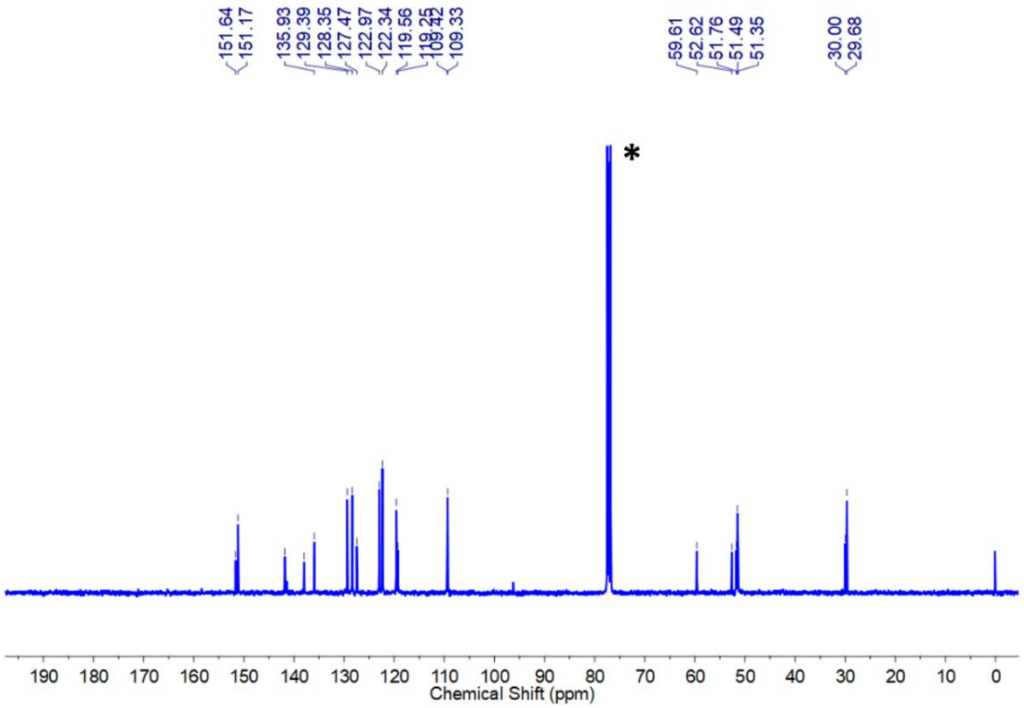

Figure S2: $^{13}C\{1H\}$ NMR spectrum of BnTBEN in $CDCl_3$ at 100 MHz. (* peak for solvent).

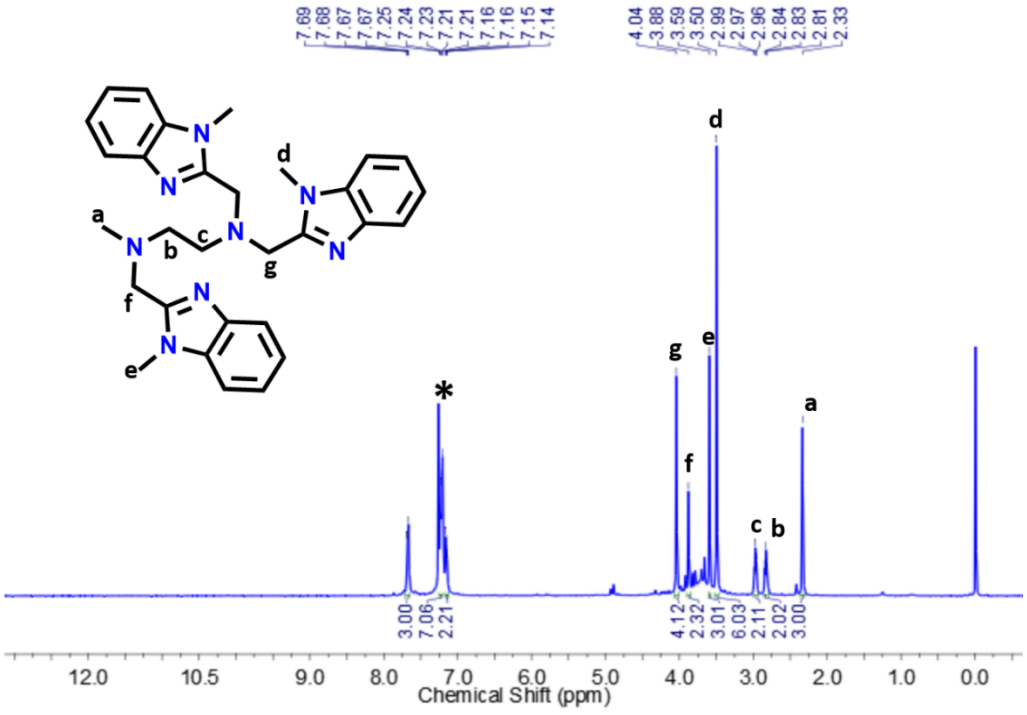

Figure S3: ^{1}H NMR spectrum of MeTBEN in $CDCl_3$ at 400 MHz. (* peak for solvent).

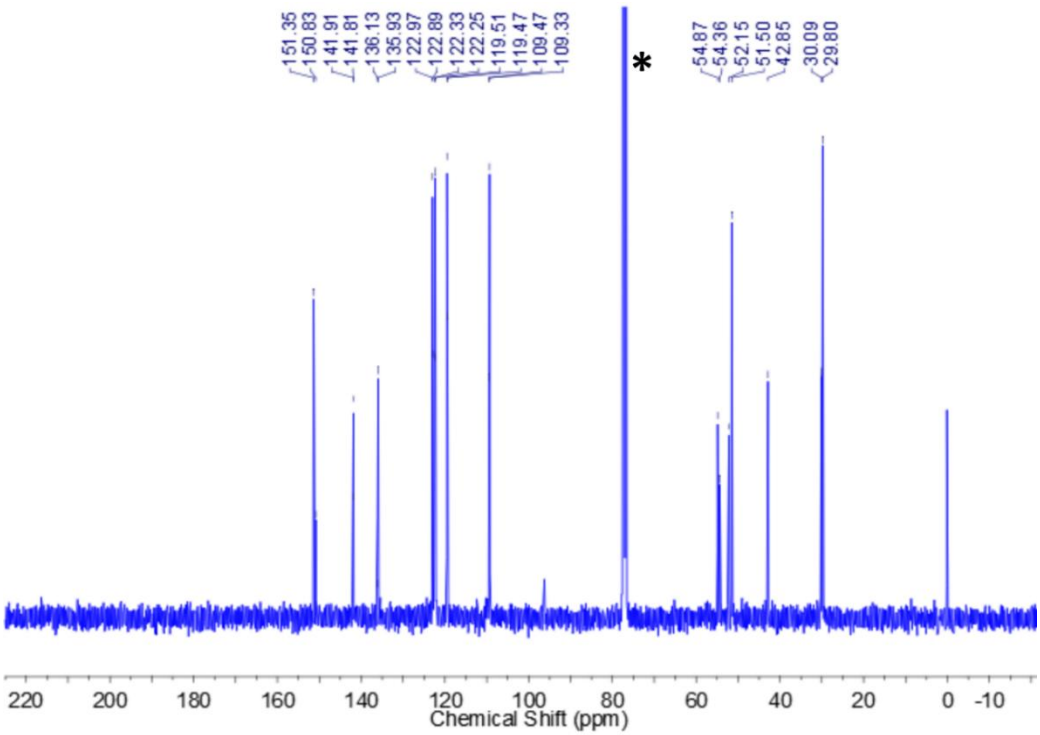

Figure S4: $^{13}C\{1H\}$ NMR spectrum of MeTBEN in $CDCl_3$ at 100 MHz. (* peak for solvent).

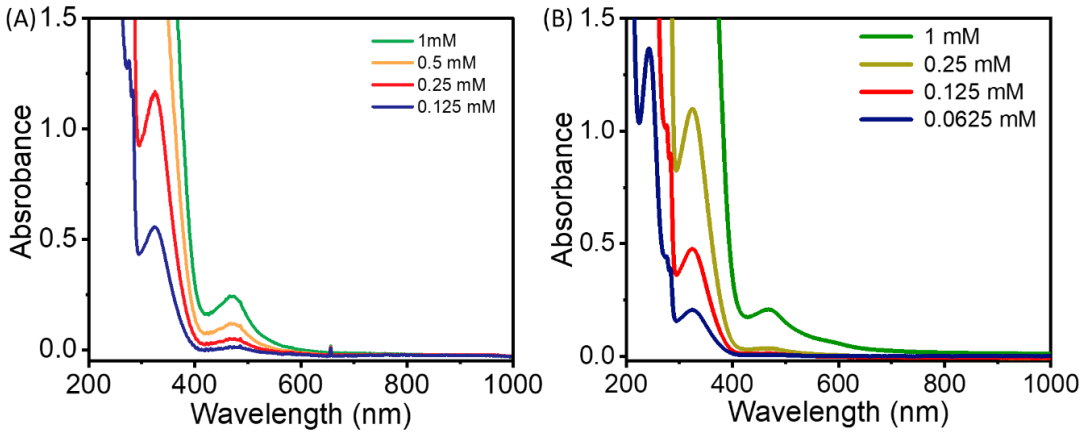

Figure S5: UV/Vis absorption spectra of (A) $[Ru^{II}(BnTBEN)(NCCH_3)](PF_6)_2$ **1** recorded at different concentrations (blue) 0.125 mM, (red) 0.25 mM, (orange) 0.5 mM, (green) 1 mM and (B) $[Ru^{II}(MeTBEN)(NCCH_3)](PF_6)_2$ **2** recorded at different concentrations (blue) 0.0625 mM, (red) 0.125 mM, (orange) 0.25 mM, (green) 1 mM in CH_3CN at room temperature.

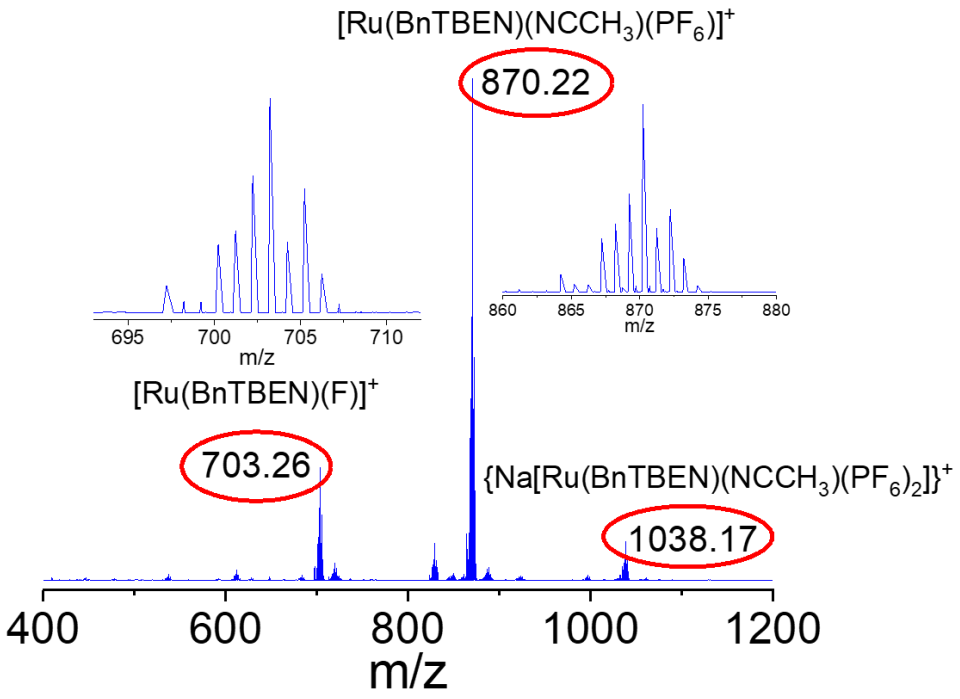

Figure S6: Positive mode ESI-mass spectrum of **1** in CH_3CN.

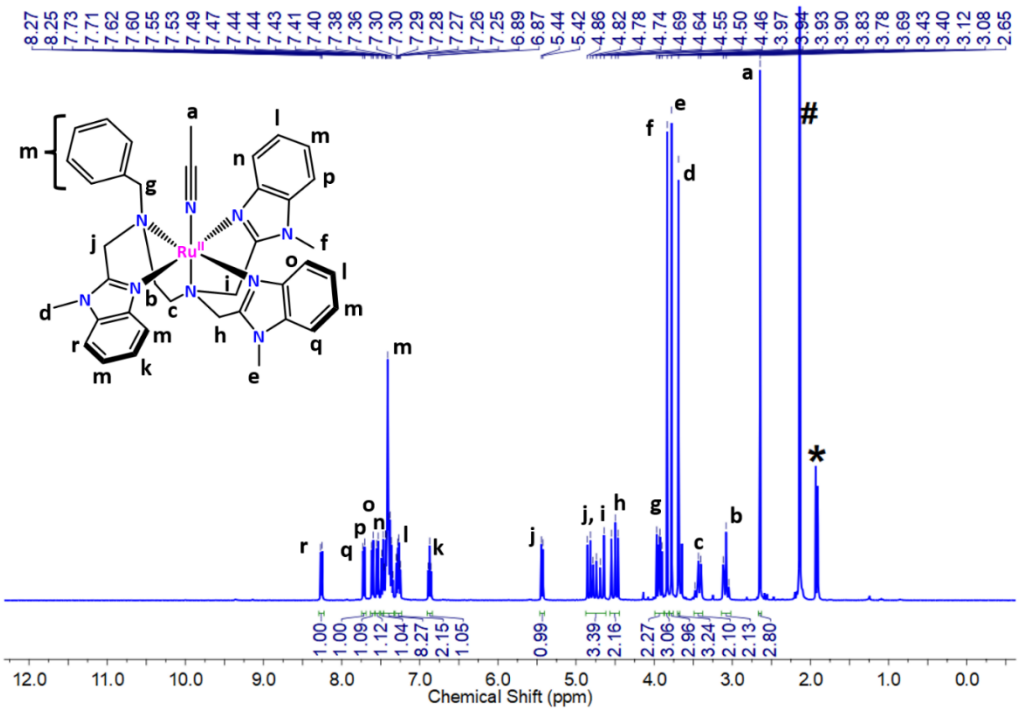

Figure S7: ^1H NMR spectrum of **1** in CD_3CN at 400 MHz. (* peak for solvent, # peak for H_2O).

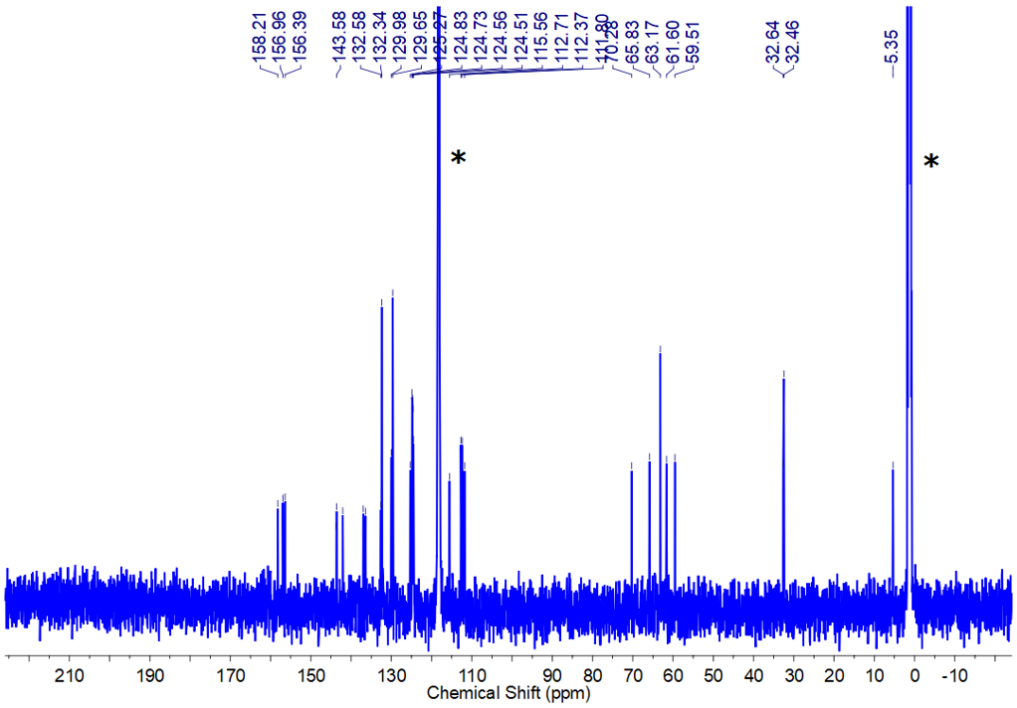

Figure S8: $^{13}C\{1H\}$ NMR spectrum of **1** in CD_3CN at 125 MHz. (* peak for solvent).

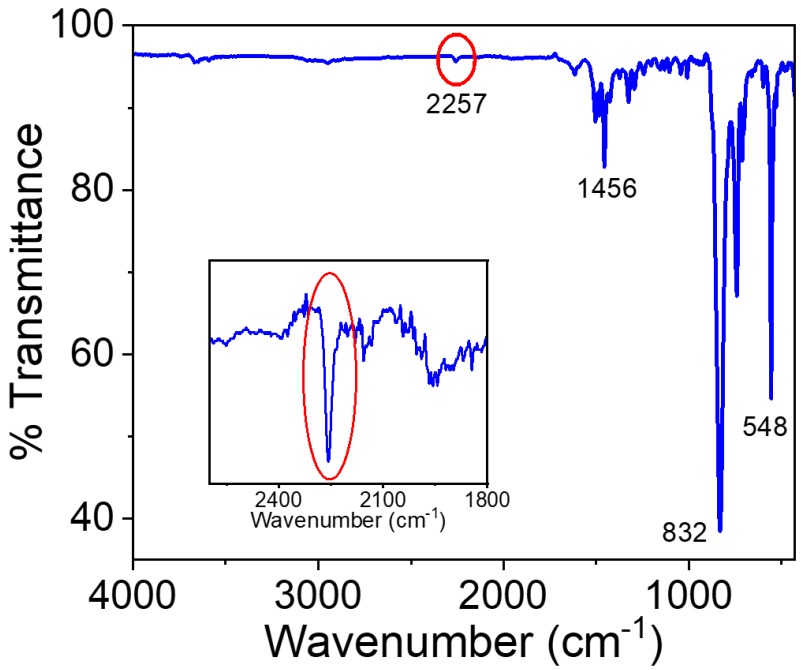

Figure S9: Solid-state FT-IR spectrum of **1** on KBr pellet. The band at 2257 cm^{-1} is originated from the bound acetonitrile ligand.

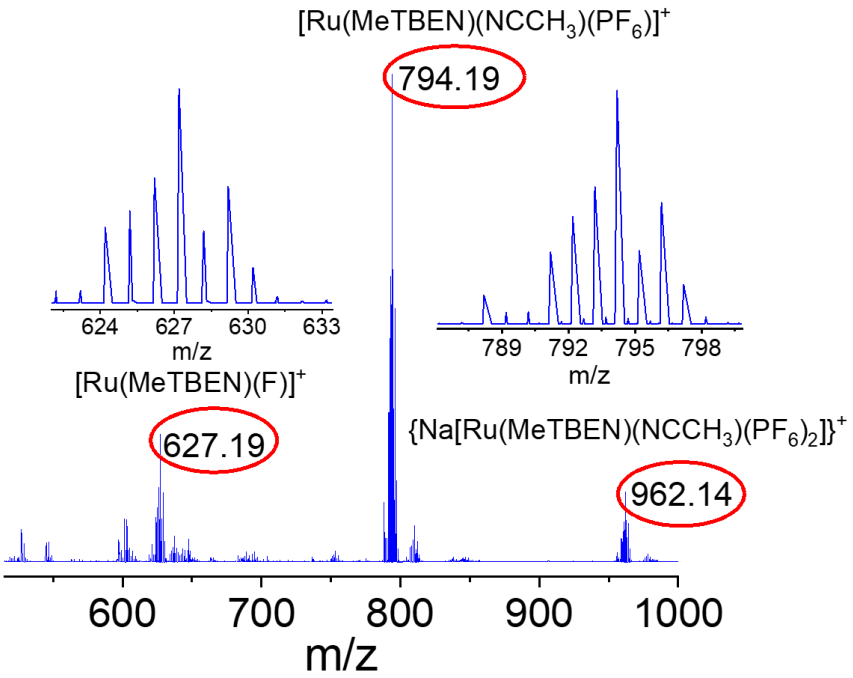

Figure S10: Positive mode ESI-mass spectrum of **2** in CH_3CN.

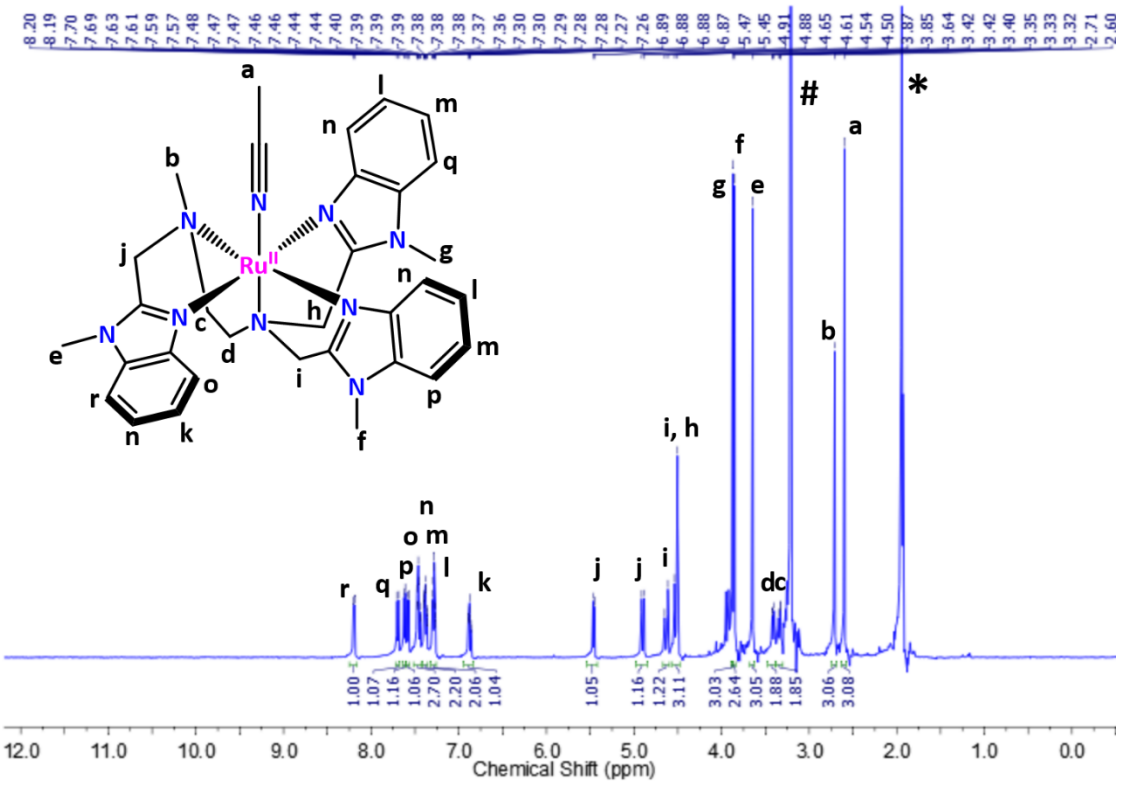

Figure S11: ^1H NMR spectrum of **2** in CD_3CN at 500 MHz. (* peak for solvent, # peak for H_2O).

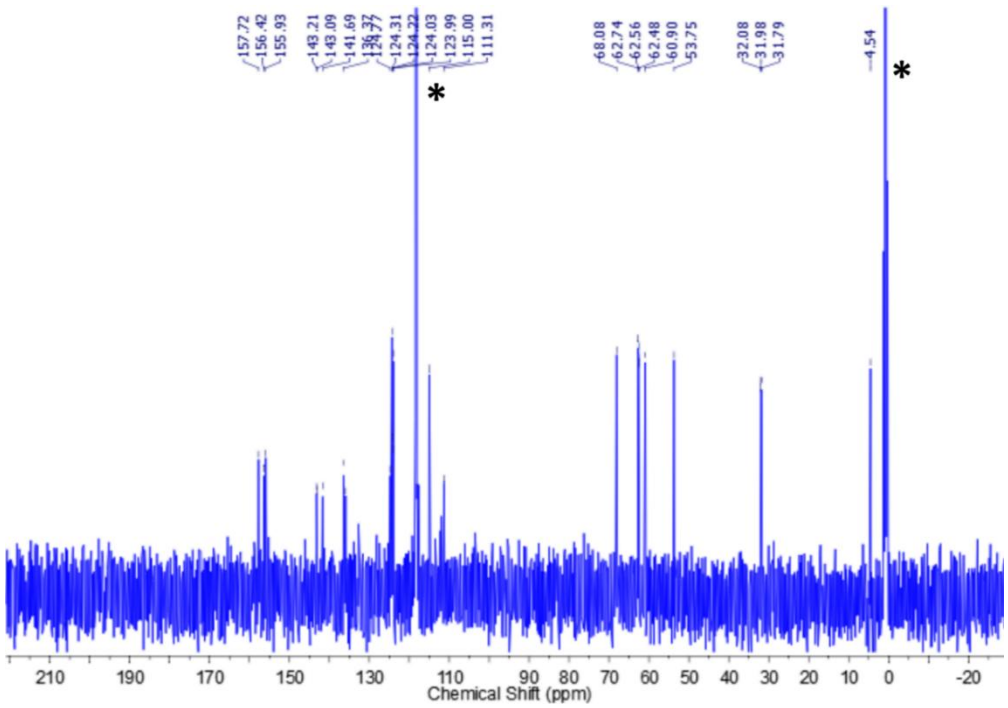

Figure S12: $^{13}C\{1H\}$ NMR spectrum of **2** in CD_3CN at 125 MHz. (* peak for solvent).

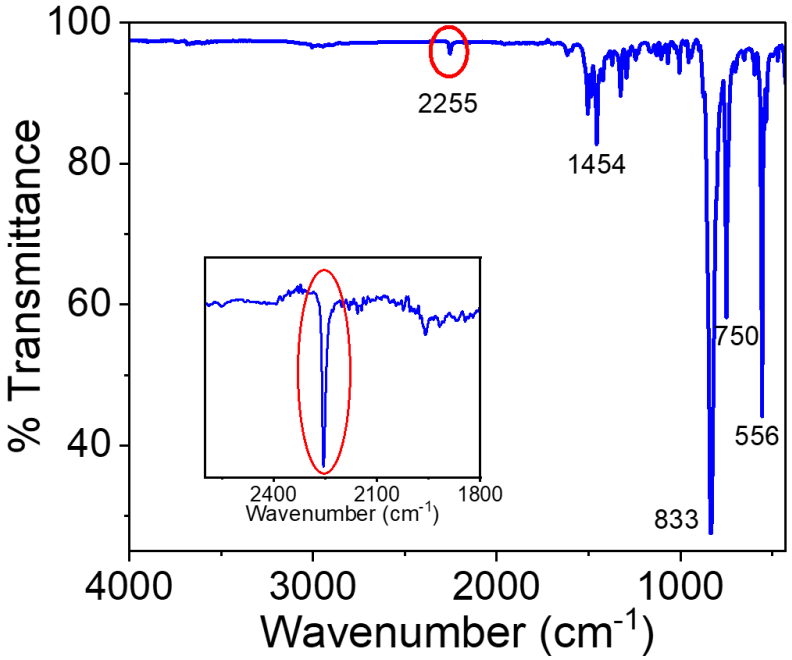

Figure S13: Solid-state FT-IR spectrum of **2** on KBr pellet. The band at 2255 cm^{-1} is originated from the bound acetonitrile ligand.

Table S1: Crystal data and structure refinement for **1** and **2**.

Identification code	**1**	**2**
Empirical formula	$C_{38}H_{41}F_{12}N_9P_2Ru$	$C_{36}H_{43}F_{12}N_{11}P_2Ru$
Formula weight	1014.81	1020.82
Temperature/K	100	100
Crystal system	monoclinic	monoclinic
Space group	C2/c	$P2_1/n$
a/Å	28.491(3)	15.2846(12)
b/Å	20.251(3)	12.4220(10)
c/Å	19.737(2)	23.5315(19)
α/°	90	90
β/°	112.506(5)	106.336(2)
γ/°	90	90
Volume/Å^3	10520(2)	4287.4(6)
Z	8	4
ρ_{calc}g/cm^3	1.281	1.581
μ/mm^{-1}	0.435	0.535
F(000)	4112.0	2072.0
Crystal size/mm^3	0.2 × 0.19 × 0.18	0.18 × 0.18 × 0.17
Radiation	MoKα (λ = 0.71073)	MoKα (λ = 0.71073)
2Θ range for data collection/°	5.448 to 56.63	4.296 to 56.594
Index ranges	-37 ≤ h ≤ 37, -26 ≤ k ≤ 26, -26 ≤ l ≤ 26	-20 ≤ h ≤ 20, -16 ≤ k ≤ 16, -31 ≤ l ≤ 31
Reflections collected	83605	65113
Independent reflections	13053 [R_{int} = 0.0789, R_{sigma} = 0.0506]	10654 [R_{int} = 0.0666, R_{sigma} = 0.0452]
Data/restraints/parameters	13053/0/626	10654/0/629
Goodness-of-fit on F^2	1.049	1.056
Final R indexes [I>=2σ (I)]	R_1 = 0.0641, wR_2 = 0.1747	R_1 = 0.0451, wR_2 = 0.0927
Final R indexes [all data]	R_1 = 0.0903, wR_2 = 0.1969	R_1 = 0.0662, wR_2 = 0.1050
Largest diff. peak/hole / e Å^{-3}	1.51/-1.11	0.5/-0.46

Table S2: Selected bond lengths for **1** and **2**.

		1	2
Atom	**Atom**	**Length/Å**	**Length/Å**
Ru(1)	N(1)	2.108(3)	2.105(3)
Ru(1)	N(2)	2.135(3)	2.149(3)
Ru(1)	N(3)	2.075(3)	2.068(3)
Ru(1)	N(4)	2.043(3)	2.058(3)
Ru(1)	N(5)	2.087(3)	2.057(3)
Ru(1)	N(6)	2.014(4)	2.022(3)

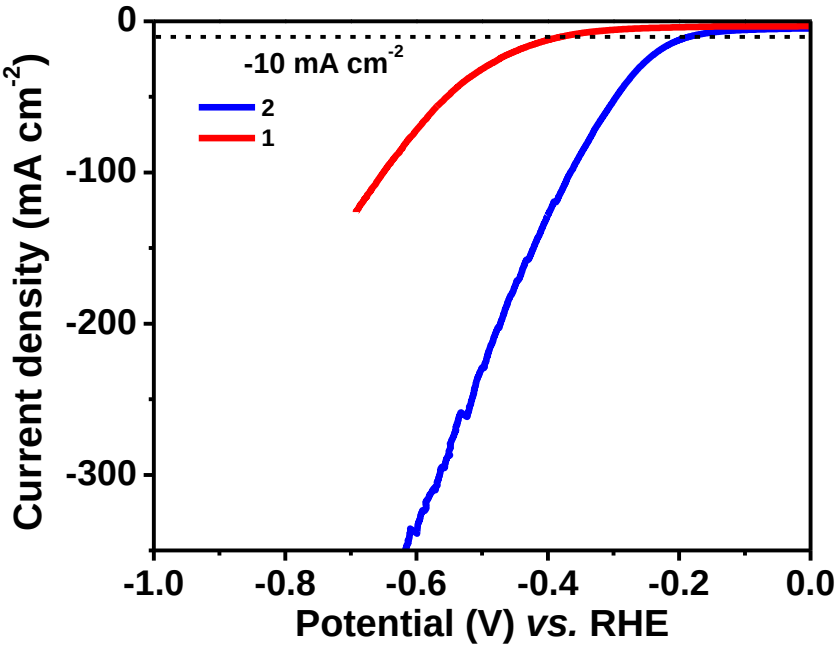

Figure S14: LSV profile for the hydrogen evolution activity of **1** and **2** in 1.0 M KOH solution.

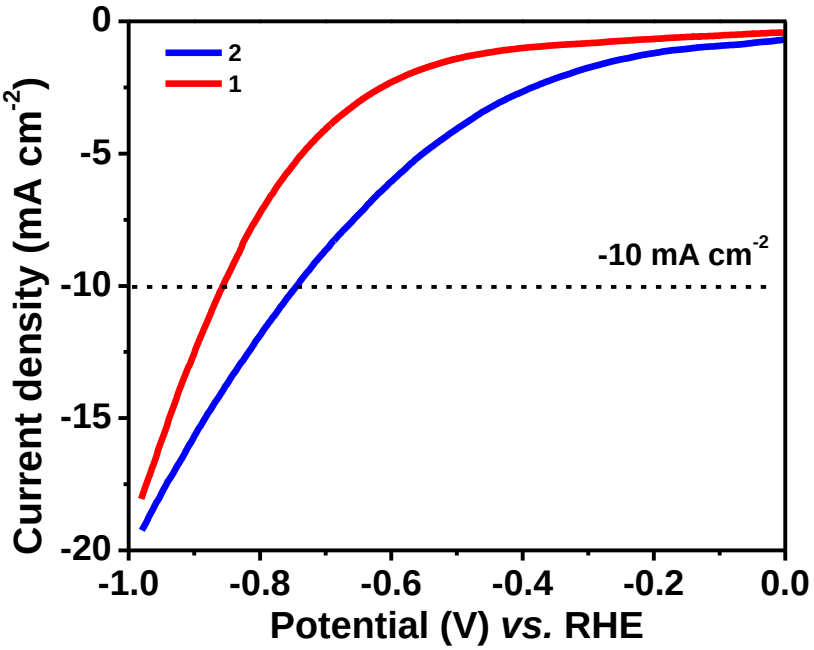

Figure S15: LSV profile for the hydrogen evolution activity of **1** and **2** in phosphate buffer.

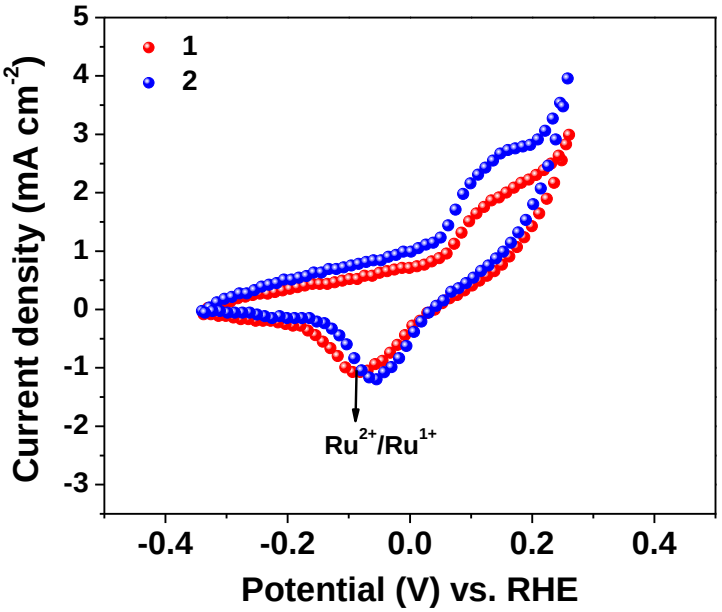

Figure S16: CV profile during HER of **1** and **2** showing the reduction peak of Ru^{2+}/Ru^{1+}.[6,7]

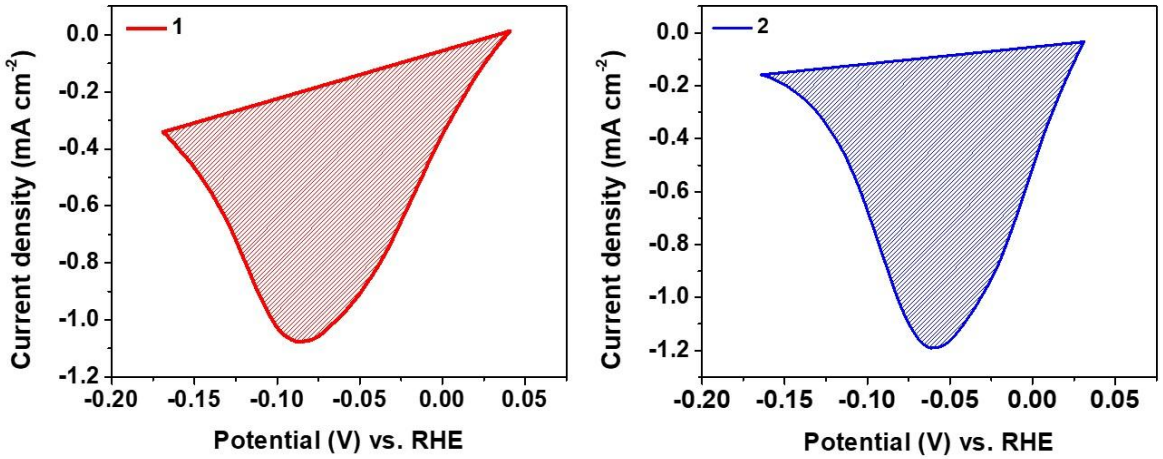

Figure S17: Reduction peaks for **1** and **2** utilized for the integration to calculate the number of active Ru-sites (scan rate 20 mV s^{-1}).[6-7]

The number of active sites for the synthesized complexes has been determined by the redox peak integration method. For this purpose, we carried out a CV at the scan rate of 20 mV s^{-1} and determined the redox peak. The reduction peak area has been integrated using the origin software. The associated charge with the reduction peak of the complexes has been calculated by dividing the reduction peak area by the scan rate. As the reduction of Ru^{2+}/Ru^{1+} is a one-electron transfer process, the associated charge has been divided by the charge of the electron to find out the number of surface-active sites.[6,7]

Equation S1:

Complex 1:

Calculated area associated with the oxidation peak = 0.02336×10^{-3} V A

Hence the associated charge was = 0.02336×10^{-3} V A / 0.02 V s^{-1}

= 1.1680×10^{-3} As

= 1.1680×10^{-3} C

Now, the number of electron transferred was = 1.1680×10^{-3} C / 1.602×10^{-19} C

= 7.29×10^{15}

The number of electrons calculated above was the same as that of the surface active site due to a single electron transfer involving the Ru^{2+}/Ru^{1+} process.
Hence,
The surface-active site that participated in HER = **7.29×10^{15}**

Complex 2:
Calculated area associated with the oxidation peak = 0.02353×10^{-3} V A
Hence the associated charge was = 0.02353×10^{-3} V A / 0.02 V s^{-1}
= 1.1765×10^{-3} As
= 1.1765×10^{-3} C
Now, the number of electron transferred was = 1.1765×10^{-3} C / 1.602×10^{-19} C
= 7.34×10^{15}
The surface-active site that participated in HER **= 7.34×10^{15}**

Equation S2:[6-7]
Calculation of Turn Over Frequency (TOF)
$TOF = (j \times N_A) / (2 \times F \times n)$
Where,
j = current density at 115 mV
N_A = Avogadro number
F = Faraday constant
n = number of active Co-sites

As complex **2** has shown the best HER activity at 115 mV overpotential, producing 10 mA cm^{-2} current density, we have calculated the TOF at 115 mV overpotential for all the complexes, resulting in the exact comparison of the TOF.

Complex 1:
TOF = $[(2.5 \times 10^{-3}) (6.023 \times 10^{23})] / [(96485) (2) (7.29 \times 10^{15})]$
TOF = 1.07 s^{-1}
Complex 2:
TOF = $[(10 \times 10^{-3}) (6.023 \times 10^{23})] / [(96485) (2) (7.34 \times 10^{15})]$
TOF = 4.25 s^{-1}

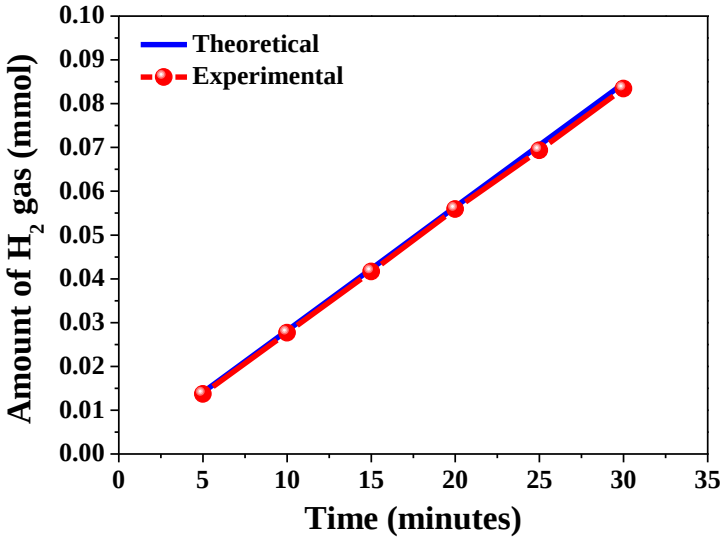

Figure S18: Theoretically and experimentally determined amount of hydrogen to determine the faradaic efficiency of **2**.

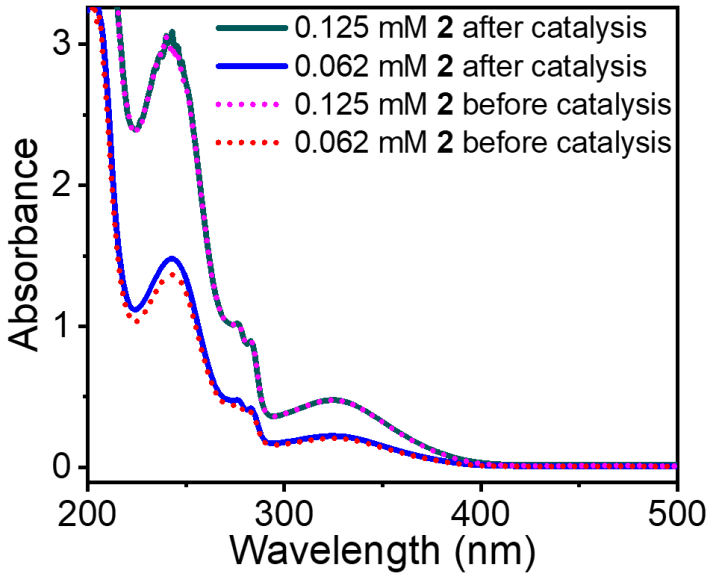

Figure S19: UV/Vis absorption spectra of **2** before electrocatalysis (red dotted line (0.062 mM) and magenta dotted line (0.125 mM)) and after electrocatalysis (blue line (0.062 mM) and green line (0.125 mM)) recorded in CH_3CN at room temperature.

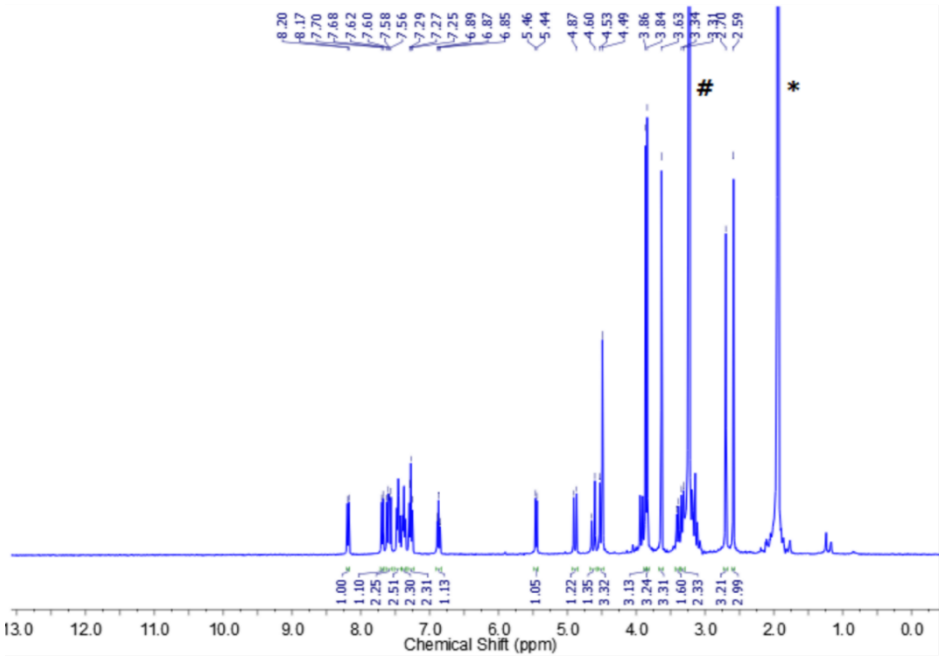

Figure S20: ^{1}H NMR spectrum of **2** in CD_3CN at 400 MHz after treatment with 0.5 M H_2SO_4 for 2 h. (* peak for solvent, # peak for H_2O).

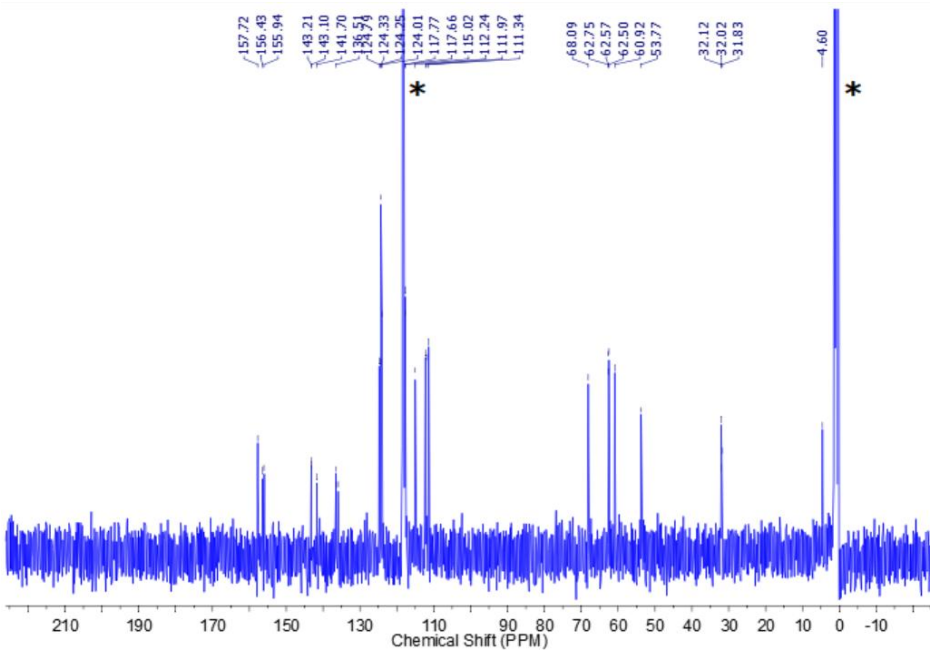

Figure S21: ^{13}C{1H} NMR spectrum of **2** in CD_3CN at 400 MHz after treatment with 0.5 M H_2SO_4 for 2 h. (* peak for solvent).

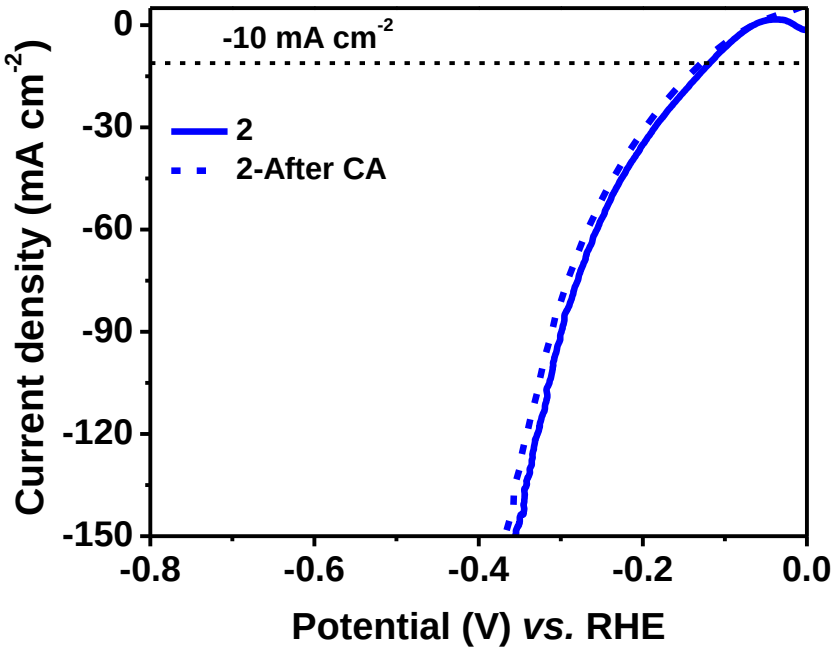

Figure S22: LSV profile of **2** for HER after-CA stability test in acidic medium.

References:

1. O. V. Dolomanov, L. J. Bourhis, R. J. Gildea, J. A. K. Howard and H. Puschmann, *J. Appl. Crystallogr.*, 2009, **42**, 339–341.

2. G. M. Sheldrick, *Acta Crystallogr. Sect. A: Found. Adv.*, 2015, **71**, 3–8.

3. G. M. Sheldrick, *Acta Crystallogr. Sect. C: Struct. Chem.*, 2015, **71**, 3–8

4. K. Vechalapu, R. Kumar, N. Chatterjee, S. Gupta, S. Khanna, P. Y. Thimmappa, S. Senthil, R. Eerlapally, M. B. Joshi, S. K. Misra, A. Draksharapu, and D. Allimuthu, *iScience,* 2024, **27***,* 109899.

5. R. Kumar, A. Awasthi, S. Gupta, R. Eerlapally and A. Draksharapu, *Dalton Trans.*, 2022, **51**, 12848–12854.

6. Y. Arya, T. Ansari, S. K. Bera, S. Panda, A. Indra and G. K. Lahiri, *Chem. Commun.*, 2024, **60**, 6011-6014.

7. S. Dey, B. Singh, S. Dasgupta, A. Dutta, A. Indra, G. K. Lahiri, *Inorg. Chem.*, 2021, **60**, 9607–9620.